Peer-reviewed version available at Nanomaterials 2019, 9, 1490; doi:10.3390/nano9101490

Article

Using Pd Doped γ-Graphyne to Detect Dissolved Gases in Transformer Oil: A Density Functional Theory Investigation

Xiaoxing Zhang [1,3], Rongxing Fang[1], Dachang Chen [2,*] and Guozhi Zhang [1]

[1] Hubei Key Laboratory for High-efficiency Utilization of Solar Energy and Operation Control of Energy Storage System, Hubei University of Technology, Wuhan, 430068, China; xiaoxing.zhang@outlook.com (X.Z.); 1508912621@qq.com (R.F.); 980064212@qq.com (G.Z.);
[2] School of Electrical Engineering and Automation, Wuhan University, Wuhan 400044, China; chendachang@163.com (D.C.);
[3] State Key Laboratory of Power Transmission Equipment & System Security and New Technology, Chongqing University, Chongqing 400044, China.
* Correspondence: chendachang@163.com

Abstract: To realize high response and selectivity gas sensor in detecting dissolved gases in transformer oil, in this study, the adsorption of four kinds of gases (H_2, CO, C_2H_2 and CH_4) on Pd-graphyne as well as the gas sensing properties evaluation were investigated. The energetically favorable structure of Pd doped γ-Graphyne was first studied, including the comparison of different adsorption sites and discussion of electronic properties. Then, the adsorption of these four molecules on Pd-graphyne was explored. The adsorption structure, adsorption energy, electron transfer and electron distribution, the band structure and density of states were calculated and analyzed. The results show that the Pd atom prefers to be adsorbed on the middle of three C≡C bonds and the band gap is smaller. The CO adsorption exhibits the largest adsorption energy and electron transfer and brings obvious change to the structure and electron properties to Pd-graphyne. Because of the conductance decrease after adsorption CO and acceptable recovery time at high temperature, the Pd-graphyne can be promising gas sensing materials to detect CO with high selectivity. This work offers theoretical support for the design of nanomaterials based gas sensor using novel structure for industrial application.

Keywords: Pd doped graphyne; Dissolved gases; adsorption; density functional theory (DFT)

1. Introduction

These years, 2D materials have attracted much attentions after the successfully synthesis of graphene by micromechanical exfoliation in 2004 [1]. Because of the excellent physical and chemical properties of graphene obtained by a large number of researches, including high surface area and surface activity, high thermal conductivity and good heat dissipation, sensitive light response and gas/ion response, graphene has broad application value and development space [2-4]. Because of the zero value of band gap, the difficulty operating the band gap restricts the wide use in industrial process. Based on this, several emerging 2D materials have been exploited, including transition metal dichalcogenides (TMDs) [5,6], isomer of graphene [7], metal carbides and nitrides [8], 2D metal-organic framework [9] etc. Because of the more flexible band structure, these materials could have more promising application in fields of optical and electronical devices.

Among numerous 2D carbon allotropy, graphyne (GY) remains one of the most popular monolayer material [10-12]. Two most popular structures, the γ-graphyne (γ-GY)/ graphdiyne (GDY) both have sp^2 and sp hybridized carbon atoms. The difference is that, in γ-GY, only one C-C triple

bond is between two hexagonal carbon rings while two triple bonds locate between two rings in GDY [10-12]. Former studies have proved that several structure of graphyne is physically and chemically stable using theoretical method, such as α-graphyne (α-GY), β-graphyne (β-GY), 6,6,12-graphye [11] etc. And graphdiyne (GDY) was the first one reported to be synthesized in experiment [13]. However, although γ-GY has not been prepared practically, several theoretical studies have shown that it has promising usage in field of catalysis, energy storage, gas/ion sensor and electronic/optical devices.γ-GY can be a promising catalyst for oxygen reduction reaction (ORR), nitrogen reaction reduction (NRR) etc. After the doping of metal atom or non-metal atom, the modified graphyne has excellent catalytic performance and can be used as single-atom catalytic material in the future [14,15]. As to the adjustment of physical properties of γ-GY such as electronic and magnetic properties, the introduction of impurity atom and surface defect is also an effective way [16-19]. The doping of metal atom cluster is also a feasible method to adjust the surface activity and electronic properties [20-22]. The GY can also be a promising gas sensing material in many fields. Pristine GY has been proved that it has weak chemical interactions with most of the common gas molecules such as CO, CH_4, CO_2, NH_3, and NO etc [23,24]. and the doping of Mn atom can obviously strengthen the chemical interactions between these molecules and γ-GY surface [24]. For gas detection of CO molecule, to improve the weak response, the substitution doping of B and N atom makes GY more sensitive to CO [25]. For detection of NH_3, doping main group atom such as Si can significantly reduce the recovery time [26]. The substitution doping of B atom can also enhance the gas sensing properties to several inorganic small molecules such as NO, NO_2 and organic molecules including [27,28]. The doping of noble atom is also proved to obviously enhance the chemical interactions between CO and γ-GY [29]. Based on the several theoretical study of GYe as gas sensing materials, the pristine GY exhibits weak chemical interactions with most of the small gas molecules and to enhance the gas sensing properties, doping impurity atom or introducing adatom on the surface is advisable and choosing appropriate doping is essential for selectivity of GY based sensing materials.

High voltage equipment has been widely used in power station, transformer substation and power distribution station etc. To guarantee the operation status of these equipments such as transformers using oil-paper insulation and gas-insulated-switchgear (GIS) using SF_6 gas as insulating medium, detecting impurity gases in these equipments using gas sensor has been widely studied. For the detection of SF_6 decompositions, several 2D materials have been explored and surface modification including doping transition metal atom or metal oxide are feasible for enhance the chemical interactions between the SF_6 decompositions and sensing materials [30-39]. And several impurity gases will emerge and dissolve in the oil in transformer after insulation fault happen, such as CO, H_2, C_2H_2, CH_4, C_2H_6, and C_2H_4 etc. So, dissolved gas analysis (DGA) method is essential for equipment inspection. In view of this, several sensing materials have been studied to detect these kinds of molecules and evaluated the gas sensing properties, including metal oxide [40-43], TMDs [44-46]. However, the selectivity, the enhancement of the sensitivity should be further considered. In this regard, due to the high surface activity of γ-GY, and the emerge active sites caused by the introduction of Pd atom [40,41,43], in this study, we proposed a DFT study of four typical dissolved gases in transformer oil (H_2, CO, C_2H_2, CH_4) adsorbed on Pd doped γ-GY. Firstly, the adsorption of one Pd atom on γ-GY was discussed and the most energetically favorable structure of Pd-GY was found. Then, the adsorption of gas molecules on the Pd-GY was investigated and the adsorption energy, electron transfer and electronic properties were discussed in detail. Finally, the different responses to these gases were evaluated. We believe this study can provide theoretical basis for graphyne based nanomaterials to detect dissolved gases in oil and guidance for future development of nanomaterial-based gas sensor in many fields.

2. Methods

All the adsorption of Pd atom and gas molecule on γ-GY are calculated in $Dmol^3$ module [47]. The Perdew-Burke-Ernzerhof function (PBE) approached by generalized gradient approximation (GGA) was chosen for correction of the exchange-correlation functional [48,49]. The total energy, band structure and density of states (DOS) were also calculated using GGA-PBE approximation

method. The double numerical plus polarization (DNP) was considered as the basis set for all the calculations and the DFT semi-core pseudopotential (DSSP) was selected to handle the electrons, that is, the norm-conserving pseudopotential was applied for calculating the core electrons to improve the calculation efficiency. The long-range interactions derived from the Van der Walls force was calculated using the DFT-D2 method, proposed by Grimme [50]. A large enough cutoff radius of 4.5 Å was set and this value remained unchanged in this study. All the geometric optimizations between the two steps were carried out using a convergence criterion of 1×10^{-5} Ha for energy convergence, 0.002 Ha/Å for force convergence, and 0.005 Å for displacement convergence. A k-point sample in Monkhorst-Pack grid of 4×4×1 was used for geometric optimization while a more accurate k-point was considered in electronic properties with a Gaussian smearing of 0.005 Ha [51]. The binding energy (E_{ads}) was calculated using the following equation:

$$E_{bind} = E_{Pd-graphyne} - E_{graphyne} - E_{Pd\ atom} \quad (1)$$

where $E_{Pd\text{-}graphyne}$, $E_{graphyne}$ *and* $E_{Pd\ atom}$ are the total energy of Pd-graphene, pristine graphyne monolayer and isolated Pd atom. After the adsorption of one Pd atom, the electron transfer was obtained using the Hirshfeld analysis method [52]:

$$Q = -\int\left(\frac{\rho_0(r)}{\sum\rho_0'(r)}\right)\bullet\left(\rho(r)-\sum\rho_0'(r)\right)dr \quad (2)$$

where $\rho(r)$ is the total electron density of the selected structure and $\rho_0(r)$ represents the electron density of every atom if separated respectively. $\sum\rho0'(r)$ is the sum of $\rho0(r)$.

The adsorption sites of Pd atom were shown in Figure 1 and considering all the structure of different adsorption sites, the structure with the largest binding energy was chosen for gas adsorption. The adsorption energy of one gas molecule on Pd-graphyne is defined as:

$$E_{ads} = E_{Pd-graphyne/gas} - E_{Pd-graphyne} - E_{gas} \quad (3)$$

where $E_{Pd\text{-}graphyne/gas}$, $E_{Pd\text{-}graphyne}$ *and* E_{gas} are the total energy of the structure of gas molecule adsorbed on Pd-graphene, Pd-graphyne before adsorption and isolated gas molecule. All the electron transfers between the gas molecule and Pd-graphyne are also obtained based on the Hirshfeld analysis method. When the electron transfer Q_T is negative, it demonstrates that the gas molecule extract electrons from Pd-graphyne and if Q_T is positive, the gas molecule transfers electrons to Pd-graphyne. To make a deeper learning of the electron transfer, the electron density difference between the molecule and Pd-graphyne can be obtained after calculating the electron density as follow:

$$\Delta\rho = \rho_{Pd-graphyne/gas} - \left(\rho_{Pd-graphyne} + \rho_{gas}\right) \quad (4)$$

where $\rho_{Pd\text{-}graphyne/gas}$, $\rho_{Pd\text{-}graphyne}$ and ρ_{gas} are the total electron density of Pd-graphyne after adsorbing molecule, Pd-graphyne before adsorption and isolated molecule, respectively. The purple region and red region are the electron accumulation region while the green region and blue region represent the electron depletion.

The band structure, the total density of states (TDOS) and the partial density of states (PDOS) were also compared before and after gas adsorption

3. Results and discussion

3.1. The structure of Pd-graphyne and dissolved gas in transformer oil

The calculated lattice parameter of γ-GY in this study is 6.89 Å×6.89 Å, which highly matches the former results [27,53]. We built a 2×2 super cell and put one Pd atom on the surface with different adsorption sites. The stoichiometric proportion of Pd and C is 1:48. The adsorption sites of Pd on the γ-GY surface is shown in Figure 1, including two hollow sites (H1, H2) and three bridge sites (B1, B2 and B3). The initial five structures of Pd-graphyne are fully geometric optimized. The optimized structures are shown in Figure 2 and the summary of binding energy and electron transfer are listed

Peer-reviewed version available at Nanomaterials 2019, 9, 1490; doi:10.3390/nano9101490

in Table 1. According to the comparison of binding energy, it can be seen that the adsorption on H1 site exhibits the largest adsorption energy indicating the most energetically favorable structure of one Pd atom on γ-GY. In Figure 2(a), the Pd atom locates in the middle of three C≡C bonds. The distance between Pd and one sp hybridized C atom is about 2.10 Å. Another point should be noted that the Pd atom is not totally in the plane of γ-GY, but it extrudes from the surface by about 0.057 Å. The binding energy of the Pd on H1 site is −2.45 eV with an electron transfer from Pd atom to γ-GY of +0.363 e. The adsorbed Pd atom is positively charged. The adsorption on B3 site exhibits the second largest adsorption energy while other adsorption energies are smaller. Based on the comparison of binding energy, we only chose the structure with the largest binding energy for further discussion of electronic properties and gas adsorption.

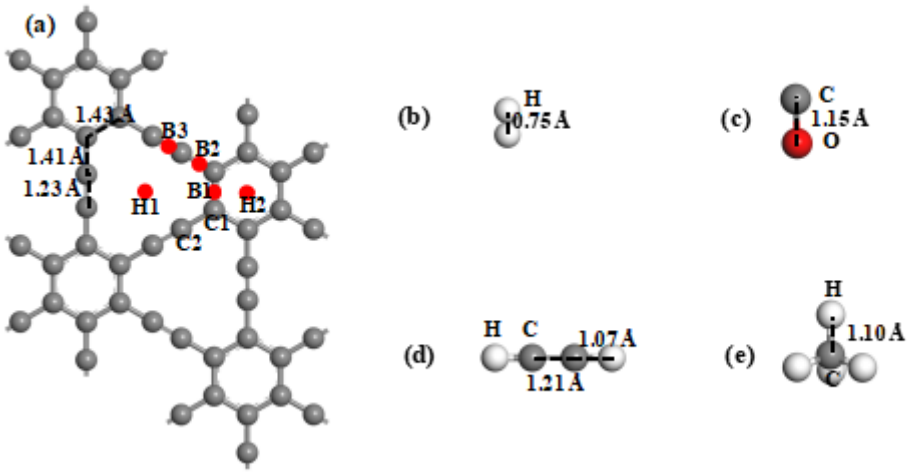

Figure 1. Geometric structures of: (**a**) pristine graphyne with different adsorption sites; (**b**) H_2; (**c**) CO; (**d**) C_2H_2; (**e**) CH_4.

Table 1. Binding energy and electron transfer of one Pd atom on graphyne monolayer.

Adsorption site	E_{bind} (eV)	Q_T (e)
H1 site	−2.45	+0.363
H2 site	−1.08	+0.323
B1 site	−1.59	+0.344
B2 site	−1.52	+0.315
B3 site	−1.76	+0.273

The band stricture and DOS of pristine γ-GY and Pd-graphyne obtained by PBE method are shown in Figure 3. The pristine γ-GY has a direct band structure with 0.42 eV band gap at Gamma point. This value is very similar with other studies (0.43 eV in ref. [21] and 0.435 eV in ref. [54]). The TDOS also shows a gap near 0 eV. It should be noted that the Fermi-level (0 eV) in Dmol^3 module is set at the highest occupied state and thus the imaginary line is at the middle of the highest occupied peak in Figure 3(a). So, the non-zero value at 0 eV is mainly because of the peak broaden. After the doping of Pd atom, the band structure also shows direct band gap and the value decreases to 0.33 eV. The Pd atom mainly introduces several impurity states near −2.5 eV to 0 eV. The Pd atom also slightly changes the band distribution near 0 eV and thus decrease the band gap. We only consider the adsorption of gas molecule on the structure in Figure 2(a) in the next section.

The structure of four kinds of gas molecule are shown in Figure 1(b) to (e). The H_2 and CO are diatomic molecules and the C atoms in C_2H_2 are sp hybridized while the C atom in CH_4 is sp^3 hybridized. The structures well conform to our previous study [44-46]. For the initial adsorption structure, we considered two adsorption directions of H_2 over the Pd atom (H_2 parallel to the surface and H_2 vertical to the surface), two adsorption directions of CO over the Pd atom (C atom downward

and O atom downward), one adsorption directions of C_2H_2 (the C≡C bond right above the Pd atom), two adsorption directions of CH_4 (one H atom downward and three H atoms downward). Only the structures with the largest adsorption energy of each gas molecule were chosen for exploration of electronic properties.

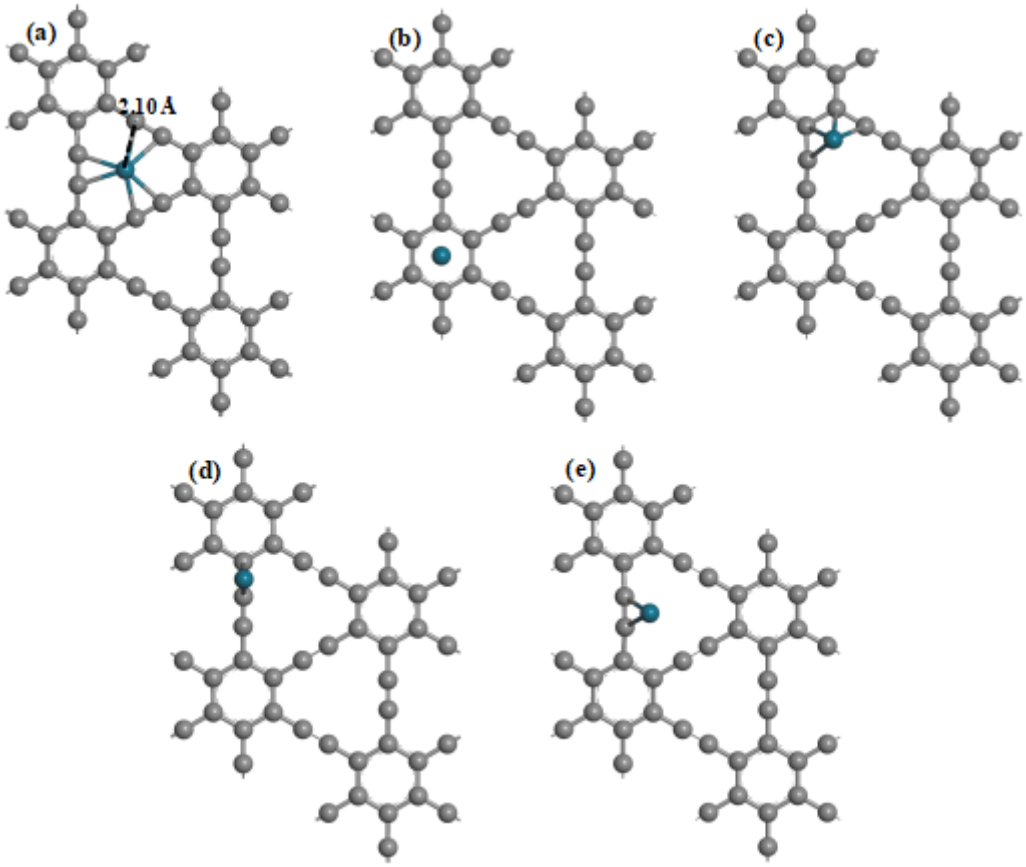

Figure 2. Optimized geometric structures of one Pd atom adsorbed on graphyne: (**a**) H1 site; (**b**) H2 site; (**c**) B1 site; (**d**) B2 site; (**e**) B3 site.

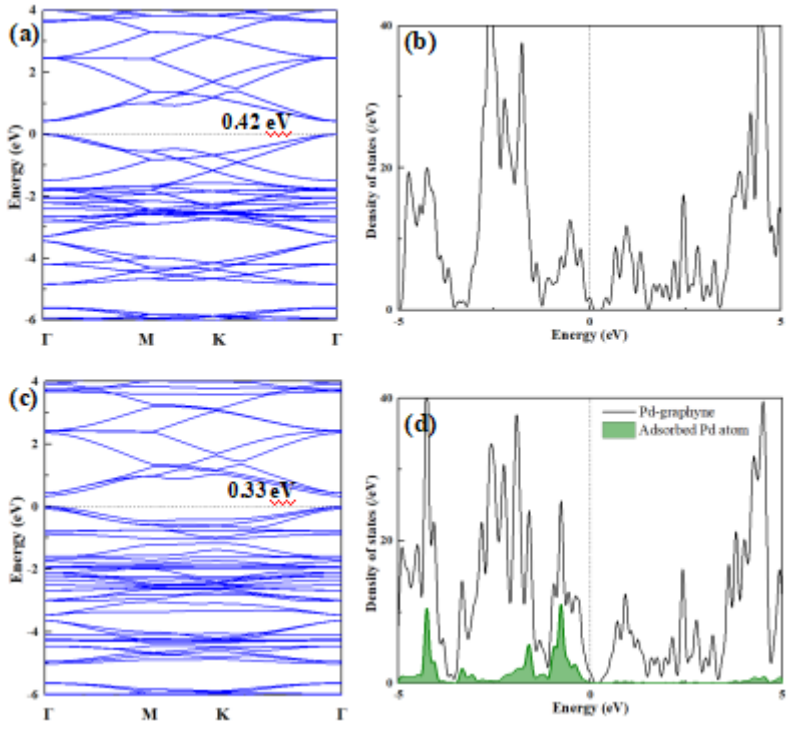

Figure 3. (**a**) Band structure and (**b**) TDOS of pristine graphyne; (**c**) Band structure and (**d**) TDOS of Pd-graphyne and PDOS of adsorbed Pd atom.

3.2. Adsorption of gas molecule on Pd-graphyne

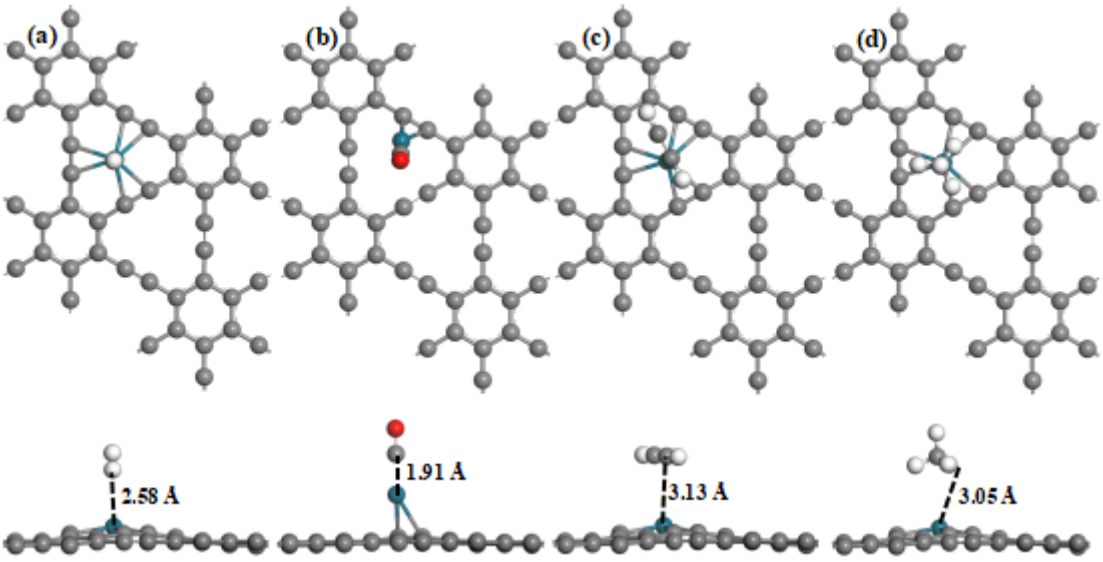

Figure 4. Optimized geometric structures of four kinds of molecule adsorbed on Pd-graphyne: (**a**) H_2 adsorption; (**b**) CO adsorption; (**c**) C_2H_2 adsorption; (**d**) CH_4 adsorption.

Table 2. Adsorption energy and electron transfer of H_2, CO, C_2H_2 or CH_4 adsorbed on Pd-graphyne.

Structure	E_{ads} (eV)	Q_T (e)
Pd-graphyne/H_2	−0.08	−0.059
Pd-graphyne/CO	−1.11	−0.080
Pd-graphyne/C_2H_2	−0.16	−0.015
Pd-graphyne/CH_4	−0.13	−0.063

The most energetically favorable adsorption structure of gas molecule on Pd-graphyne are shown in Figure 4, and the adsorption energy and electron transfer are listed in Table 2. The H_2 molecule prefers to be adsorbed vertically to the surface right above the Pd atom. The adsorption brings only −0.08 eV adsorption energy and −0.059 e electron transfer. The adsorption distance is 2.58 Å. The Pd atom nearly stays its former position. For the adsorption of CO, the circumstance has some differences. The C atom in CO prefers to be right above the Pd atom and the Pd atom moves from H1 site to B3 site (between one C≡C bond). The CO obtains −0.080 e from Pd-graphyne indicating the role of electron acceptor. The adsorption energy of CO on Pd-graphyne reaches −1.11 eV, which is the largest among these four molecules. The adsorption of C_2H_2 exhibits only −0.16 eV adsorption energy with very small electron transfer (−0.015 e) compared to other adsorptions. And one sp hybridized C atom is right above the Pd atom. The CH_4 adsorption has −0.13 eV adsorption energy and −0.063 e electron transfer. For the adsorption of C_2H_2 and CH_4, the adsorption distance is much larger compared to the adsorption of H_2 and CO and the position of Pd atom is unchanged. To sum up, only CO adsorption brings significant change of the structure of Pd-graphyne with much larger adsorption energy.

To make a more advanced analysis of the interactions, the electron density difference (EDD) was calculated and the results are shown in Figure 5. For the adsorption of H_2, obvious electron accumulation happens near the above H atom and between the H_2 and Pd atom while depletion

region is between two H atoms. However, the Pd-graphyne does not show obviously electron density change. The CO adsorption results in obvious change of electron distribution. Apparent electron accumulation is between the molecule and Pd atom and depletion is around Pd and between C and O atom. The electrons prefer to move between the molecule and Pd atom rather than beneath the Pd. The adsorption of C_2H_2 brings obvious electron depletion around Pd and change the electron distribution of Pd-graphyne to some extent. As to the CH_4 adsorption, only slight depletion region can be found around Pd atom. Given the different isosurface in Figure 5(b), the CO adsorption makes the largest electron redistribution and the C_2H_2 adsorption also brings the considerable change of electron density in Pd-graphyne. But other two adsorptions only result in smaller effect. The relationship of electron transfer and electronic properties after adsorption will be discussed in the next section.

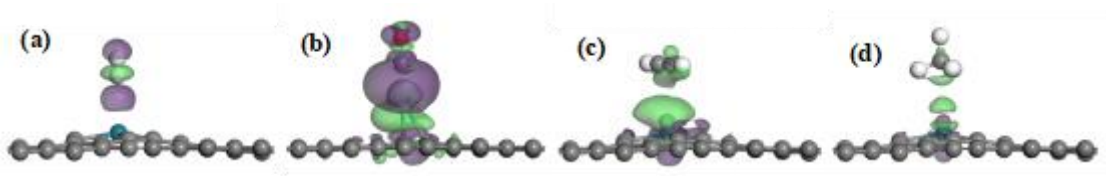

Figure 5. Electron density difference (EDD) of four kinds of molecule adsorbed on Pd-graphyne: (**a**) H_2 adsorption; (**b**) CO adsorption; (**c**) C_2H_2 adsorption; (**d**) CH_4 adsorption. The purple region denotes the electron accumulation region and the green region represents the electron depletion (the isosurface of (a), (c) and (d) is 0.005 eÅ^{-3}; the isosurface of (b) is 0.002 eÅ^{-3}).

3.3. Electronic properties of Pd-graphyne and gas sensing evaluation

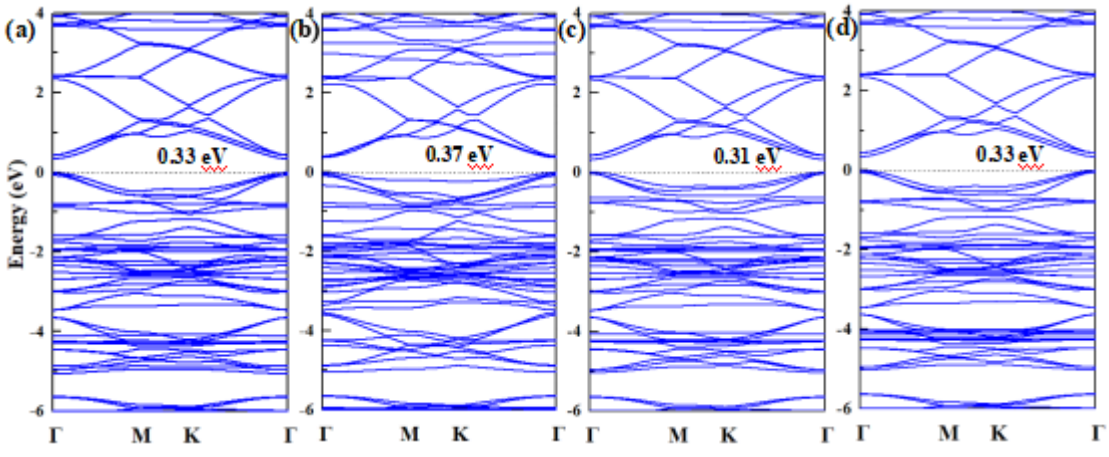

Figure 6. Band structure of (**a**) Pd-graphyne/H_2; (**b**) Pd-graphyne/CO; (**c**) Pd-graphyne/C_2H_2 and (**d**) Pd-graphyne/CH_4.

To investigate the effect to the electronic properties of Pd-graphyne, the band structure and DOS before and after adsorption were compared. The band structures of Pd-graphyne after adsorbing gas molecule are shown in Figure 6. All the band structures still show a direct band gap, but the gap values have some differences. The H_2 adsorption and CH_4 adsorption do not exhibit obvious change of the band structure. However, the CO adsorption increases the band gap while the C_2H_2 decreases it. Considering the electron distribution in Figure 5, only the CO and C_2H_2 adsorption bring obvious change in electron distribution and change the electronic properties of Pd-graphyne. As a result, the band gap changes only when CO and C_2H_2 adsorption.

To further investigate the electronic properties, the TDOS of Pd-graphyne after adsorption and PDOS of the adsorbed molecule are shown in Figure 7. For the adsorption of H_2 and CH_4, the states near Fermi-level do not exhibit obvious change. However, the adsorbed CO and C_2H_2 molecule introduce several impurity states just below The Fermi-level, and thus, these states change the

Preprints (www.preprints.org) | NOT PEER-REVIEWED | Posted: 25 September 2019 doi:10.20944/preprints201909.0286.v1

Peer-reviewed version available at Nanomaterials 2019, 9, 1490; doi:10.3390/nano9101490

electronic properties of Pd-graphyne near 0 eV and also the new band gap has some differences compared to the Pd-graphyne before adsorption. Because the CO adsorption has much shorter adsorption distance, larger adsorption energy and significant change of the structure and electron distribution, the chemical interactions between Pd atom and CO are explored using the PDOS of atomic orbitals of Pd and C atom in CO, as shown in Figure 7(e). The states between −7 eV to −6 eV consist of Pd 5s, Pd 4d and C 2p orbitals. The states between −3 eV to 0 eV are mainly Pd 4d and 5s orbitals. As to the antibonding orbitals above 0 eV, the states are composed of Pd 4d, 5p and C 2p orbitals. The obvious hybridizations of peaks near −6 eV and +3 eV between Pd and C atomic orbitals show significant chemical interactions between these two atoms. In summary, the largest adsorption energy (−1.11 eV), largest electron transfer (−0.080 e) of CO compared to other adsorptions, the significant state hybridization between Pd and C atom indicate the strong interactions between CO and Pd-graphyne.

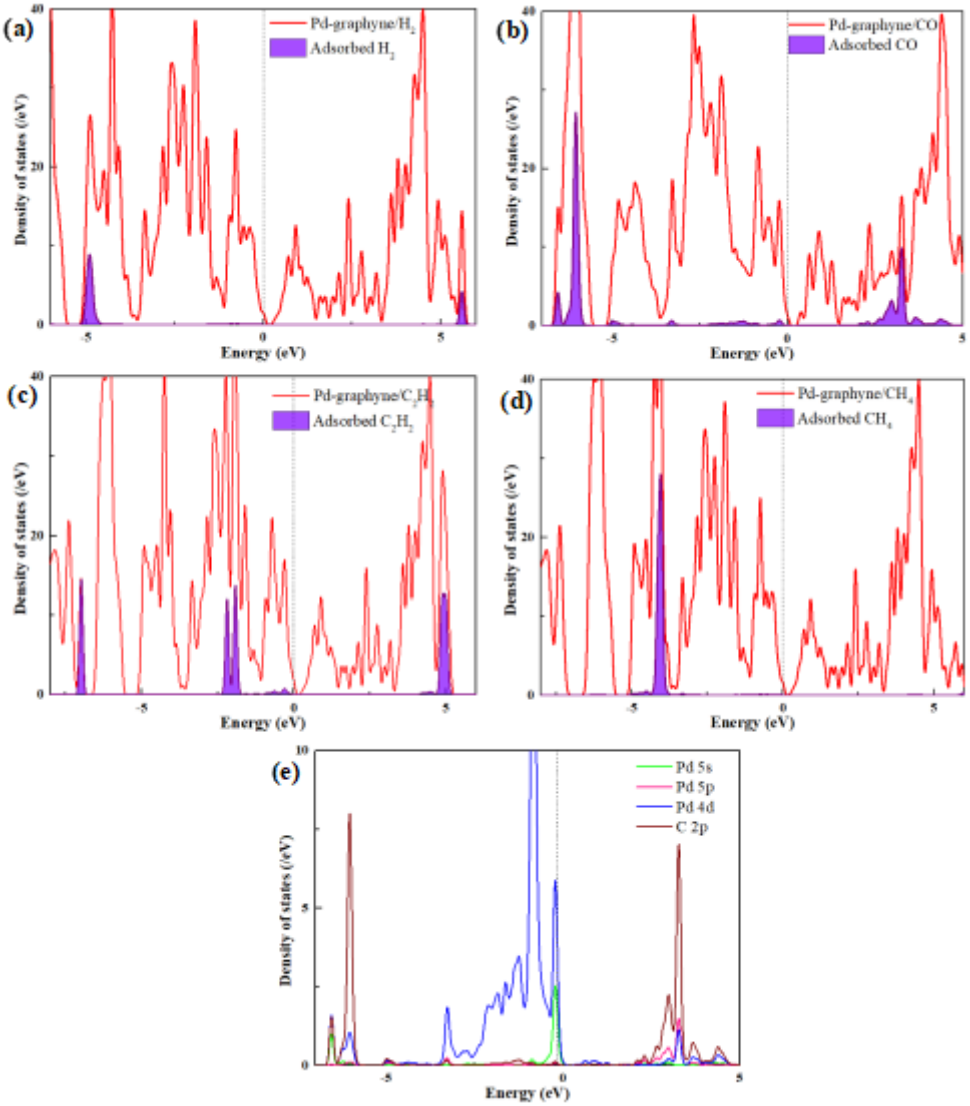

Figure 7. TDOS and PDOS of (**a**) Pd-graphyne/H_2; (**b**) Pd-graphyne/CO; (**c**) Pd-graphyne/C_2H_2; (**d**) Pd-graphyne/CH_4 and (**e**) atomic orbitals of CO adsorption.

For the gas sensing properties, the resistance type gas sensor has attracted much attention. The electrical conductivity is high affected by the band structure of the sensing materials, the change of the resistance can be evaluated by the band gap [55]:

$$\sigma \propto e^{\left(-E_g/2k_BT\right)} \quad (5)$$

where σ represents the evaluated conductance of the gas sensor, k_B is Boltzmann constant and T is the working temperature of the gas sensor. It can be seen that, in a fixed working temperature, the smaller band gap brings the larger conductance and vice versa. In this study, the band gap of Pd-graphyne is 0.33 eV and increases to 0.37 eV when adsorbing CO while decreases to 0.31 eV after C_2H_2 adsorption. As a result, the conductance experiences risen when detecting C_2H_2 and fallen when adsorbing CO. However, another point should be also considered. The recovery time of the sensor is an important aspect to evaluate the sensing properties. A very short recovery time can promote the desorption process, but the fast desorption may lead to the higher limit of detection. So the recovery time should be controlled to an acceptable range. The recovery time can be evaluated as follow [56]:

$$\tau = A^{-1} e^{(-E_{bar}/k_B T)} \quad (6)$$

where A denotes the apparent frequency factor, k_B is the Boltzmann's constant and T is the working temperature, respectively. E_{bar} is the energy barrier of the molecule desorption from the surface. Because the desorption can be seen as the inverse process of the adsorption, the absolute value of E_{bar} and E_{ads} is the same. The value of A can be evaluated as 10^{12} s^{-1}, which has the consistency with other study [57]. According to the above precondition, the desorption time of H_2, C_2H_2 and CH_4 is 2.25×10^{-11} s, 5.08×10^{-10} s, 1.58×10^{-10} s, which is much smaller than that of CO, reaching 5.92×10^{-6} s at 298K. It can be seen that, at room temperature, CO is hard to desorb from the surface but the much faster desorption of C_2H_2 may result in much higher detection limit. But if the working temperature reaches 498K, the desorption time of CO decreases to about 0.171 s, this much shorter time is suitable for CO sensing. As a result, the Pd-graphyne based gas sensor may have very good selectivity to CO at higher temperature.

4. Conclusions

This study discussed the structure and electronic properties of Pd-graphyne as well as its adsorption properties toward four typical kinds of dissolved gases in transformer oil (H_2, CO, C_2H_2 and CH_4). Pd atom prefers to be adsorbed on the H1 site with the largest binding energy (−2.45 eV) and electron transfer (+0.363 e). The introduction of Pd atom decreases the band gap and brings in impurity states just below 0 eV. Among the four types of gases, the CO adsorption brings the largest adsorption energy and electron transfer, and moreover, the Pd atom moves from H1 site to B3 site resulting in the obvious change of geometric structure and electronic properties of Pd-graphyne. The band gap becomes larger after CO adsorption while smaller after C_2H_2 adsorption. The strong chemical interactions between the Pd-graphyne and adsorbed CO are mainly attributed to the hybridizations of atomic orbitals of Pd atom and C atom in CO. The recovery properties of Pd-graphyne based gas sensor show that the recovery time is about 0.171 s for CO desorption at 498K which indicating the acceptable recovery properties of Pd-graphyne to CO at this temperature and may realize high selectivity gas sensor for CO detection.

Author Contributions: X.Z. and D.C. proposed the project and organized the manuscript. R.F. and G.Z. contributed to the theoretical simulation and analyzed the simulation results. All authors read and approved the final manuscript.

Funding: This research was funded by the National Natural Science Foundation of China under Grant 51777144.

Conflicts of Interest: The authors declare no conflict of interest.

References

1. Novoselov, K.S.; Geim, A.K.; Morozov, S.V.; Jiang, D.; Zhang, Y.; Dubonos, S.V.; Grigorieva, I.V.; Firsov, A.A. Electric field effect in atomically thin carbon films. *Science* **2004**, 306, 666.
2. Sun, P.; Wang, K.; Zhu, H. Recent developments in graphene-based membranes: Structure, mass-transport mechanism and potential applications. *Adv. Mater.* **2016**, 28, 2287-2310.
3. Huang, X.; Yin, Z.; Wu, S.; Qi, X.; He, Q.; Zhang, Q.; Yan, Q.; Boey, F.; Zhang, H. Graphene-based materials: Synthesis, characterization, properties, and applications. *Small* **2011**, 7, 1876-1902.

4. Singh, V.; Joung, D.; Zhai, L.; Das, S.; Khondaker, S.I.; Seal, S. Graphene based materials: Past, present and future. *Prog. Mater. Sci.* **2011**, 56, 1178-1271.
5. Hu, Z.; Wu, Z.; Han, C.; He, J.; Ni, Z.; Chen, W. Two-dimensional transition metal dichalcogenides: Interface and defect engineering. *Chem. Soc. Rev.* **2018**, 47, 3100-3128.
6. Tan, C.; Zhang, H. Two-dimensional transition metal dichalcogenide nanosheet-based composites. *Chem. Soc. Rev.* **2015**, 44, 2713-2731.
7. Rajkamal, A.; Thapa, R. Carbon allotropes as anode material for lithium-ion batteries. *Adv. Mater. Technol.* **2019**, 0, 1900307.
8. Naguib, M.; Mochalin, V.N.; Barsoum, M.W.; Gogotsi, Y. 25th anniversary article: Mxenes: A new family of two-dimensional materials. *Adv. Mater.* **2014**, 26, 992-1005.
9. Zhao, M.; Huang, Y.; Peng, Y.; Huang, Z.; Ma, Q.; Zhang, H. Two-dimensional metal–organic framework nanosheets: Synthesis and applications. *Chem. Soc. Rev.* **2018**, 47, 6267-6295.
10. Li, Y.; Xu, L.; Liu, H.; Li, Y. Graphdiyne and graphyne: From theoretical predictions to practical construction. *Chem. Soc. Rev.* **2014**, 43, 2572-2586.
11. Huang, C.; Li, Y.; Wang, N.; Xue, Y.; Zuo, Z.; Liu, H.; Li, Y. Progress in research into 2d graphdiyne-based materials. *Chem. Rev.* **2018**, 118, 7744-7803.
12. Sakamoto, R.; Fukui, N.; Maeda, H.; Matsuoka, R.; Toyoda, R.; Nishihara, H. The accelerating world of graphdiynes. *Adv. Mater.* **2019**, 0, 1804211.
13. Li, G.; Li, Y.; Liu, H.; Guo, Y.; Li, Y.; Zhu, D. Architecture of graphdiyne nanoscale films. *Chem. Commun.* **2010**, 46, 3256-3258.
14. Gao, X.; Zhou, Y.; Tan, Y.; Liu, S.; Cheng, Z.; Shen, Z. Graphyne doped with transition-metal single atoms as effective bifunctional electrocatalysts for water splitting. *Appl. Surf. Sci.* **2019**, 492, 8-15.
15. He, T.; Matta, S.K.; Du, A. Single tungsten atom supported on N-doped graphyne as a high-performance electrocatalyst for nitrogen fixation under ambient conditions. *Phys. Chem. Chem. Phys.* **2019**, 21, 1546-1551.
16. Kim, S.; Ruiz Puigdollers, A.; Gamallo, P.; Viñes, F.; Lee, J.Y. Functionalization of γ-graphyne by transition metal adatoms. *Carbon* **2017**, 120, 63-70.
17. He, J.; Zhou, P.; Jiao, N.; Ma, S.Y.; Zhang, K.W.; Wang, R.Z.; Sun, L.Z. Magnetic exchange coupling and anisotropy of 3d transition metal nanowires on graphyne. *Sci. Rep.* **2014**, 4, 4014.
18. Kang, B.; Shi, H.; Wang, F.-F.; Lee, J.Y. Importance of doping site of B, N, and O in tuning electronic structure of graphynes. *Carbon* **2016**, 105, 156-162.
19. Kang, B.; Ai, H.; Lee, J.Y. Single-atom vacancy induced changes in electronic and magnetic properties of graphyne. *Carbon* **2017**, 116, 113-119.
20. Chen, Z.W.; Wen, Z.; Jiang, Q. Rational design of Ag38 cluster supported by graphdiyne for catalytic co oxidation. *J. Phys. Chem. C* **2017**, 121, 3463-3468.
21. Chen, D.; Zhang, X.; Tang, J.; Cui, H.; Li, Y.; Zhang, G.; Yang, J. Density functional theory study of small Ag cluster adsorbed on graphyne. *Appl. Surf. Sci.* **2019**, 465, 93-102.
22. Seif, A.; López, M.J.; Granja-DelRío, A.; Azizi, K.; Alonso, J.A. Adsorption and growth of palladium clusters on graphdiyne. *Phys. Chem. Chem. Phys.* **2017**, 19, 19094-19102.
23. Meng, Z.; Zhang, X.; Zhang, Y.; Gao, H.; Wang, Y.; Shi, Q.; Rao, D.; Liu, Y.; Deng, K.; Lu, R. Graphdiyne as a high-efficiency membrane for separating oxygen from harmful gases: A first-principles study. *ACS Appl. Mater. Interfaces* **2016**, 8, 28166-28170.
24. Lu, Z.; Lv, P.; Ma, D.; Yang, X.; Li, S.; Yang, Z. Detection of gas molecules on single Mn adatom adsorbed graphyne: A DFT-D study. *J. Phys. D-Appl. Phys.* **2018**, 51, 065109.
25. Omidvar, A.; Mohajeri, A. Decorated graphyne and its boron nitride analogue as versatile nanomaterials for CO detection. *Mol. Phys.* **2015**, 113, 3900-3908.
26. Peyghan, A.A.; Rastegar, S.F.; Hadipour, N.L. DFT study of NH_3 adsorption on pristine, Ni- and Si-doped graphynes. *Phys. Lett. A* **2014**, 378, 2184-2190.
27. Guo, Y.; Chen, Z.; Wu, W.; Liu, Y.; Zhou, Z. Adsorption of NOx (x = 1, 2) gas molecule on pristine and B atom embedded γ-graphyne based on first-principles study. *Appl. Surf. Sci.* **2018**, 455, 484-491.
28. Nagarajan, V.; Srimathi, U.; Chandiramouli, R. First-principles insights on detection of dimethyl amine and trimethyl amine vapors using graphdiyne nanosheets. *Comput. Theor. Chem.* **2018**, 1123, 119-127.
29. Ma, D.W.; Li, T.; Wang, Q.; Yang, G.; He, C.; Ma, B.; Lu, Z. Graphyne as a promising substrate for the noble-metal single-atom catalysts. *Carbon* **2015**, 95, 756-765.

30. Chen, D.; Zhang, X.; Cui, H.; Tang, J.; Pi, S.; Cui, Z.; Li, Y.; Zhang, Y. High selectivity n-type InSe monolayer toward decomposition products of sulfur hexafluoride: A density functional theory study. *Appl. Surf. Sci.* **2019**, 479, 852-862.
31. Chen, D.; Zhang, X.; Xiong, H.; Li, Y.; Tang, J.; Xiao, S.; Zhang, D. A first-principles study of the SF_6 decomposed products adsorbed over defective WS_2 monolayer as promising gas sensing device. *IEEE Trans. Device Mater. Reliab.* **2019**, 19, 473-483.
32. Chen, D.; Zhang, X.; Tang, J.; Pi, S.; Li, Y.; Cui, Z. High Selective SO_2 Gas Sensor Based on Monolayer β-AsSb to Detect SF_6 Decompositions. *IEEE Sens. J.* **2018**, 19, 1215-1223.
33. Chen, D.; Tang, J.; Zhang, X.; Li, Y.; Liu, H. Detecting decompositions of sulfur hexafluoride using MoS_2 monolayer as gas sensor. *IEEE Sens. J.* **2018**, 19, 39-46.
34. Chen, D.; Zhang, X.; Tang, J.; Cui, Z.; Cui, H. Pristine and Cu decorated hexagonal Inn monolayer, a promising candidate to detect and scavenge SF_6 decompositions based on first-principle study. *J. Hazard. Mater.* **2019**, 363, 346-357.
35. Chen, D.; Zhang, X.; Tang, J.; Cui, Z.; Cui, H.; Pi, S. Theoretical study of monolayer $PtSe_2$ as outstanding gas sensor to detect SF_6 decompositions. *IEEE Electron Device Lett.* **2018**, 39, 1405-1408.
36. Zhang, D.; Wu, J.; Li, P.; Cao, Y. Room-temperature SO_2 gas-sensing properties based on a metal-doped MoS_2 nanoflower: An experimental and density functional theory investigation. *J. Mater. Chem. A* **2017**, 5, 20666-20677.
37. Chu, J.; Wang, X.; Wang, D.; Yang, A.; Lv, P.; Wu, Y.; Rong, M.; Gao, L. Highly selective detection of sulfur hexafluoride decomposition components H_2S and SOF_2 employing sensors based on tin oxide modified reduced graphene oxide. *Carbon* **2018**, 135, 95-103.
38. Cui, H.; Zhang, X.; Li, Y.; Chen, D.; Zhang, Y. First-principles insight into Ni-doped Inn monolayer as a noxious gases scavenger. *Appl. Surf. Sci.* **2019**, 494, 859-866.
39. Cui, H.; Liu, T.; Zhang, Y.; Zhang, X. Ru-InN Monolayer as a Gas Scavenger to Guard the Operation Status of SF_6 Insulation Devices: A First-Principles Theory. *IEEE Sens. J.* **2019**, 19(13), 5249-5255.
40. Zhang, Q.; Zhou, Q.; Lu, Z.; Wei, Z.; Xu, L.; Gui, Y. Recent advances of SnO_2-based sensors for detecting fault characteristic gases extracted from power transformer oil. *Front. Chem.* **2018**, 6, 364-364.
41. Fan, J.; Wang, F.; Sun, Q.; Ye, H.; Jiang, Q. Application of polycrystalline SnO_2 sensor chromatographic system to detect dissolved gases in transformer oil. *Sens. Actuator B-Chem.* **2018**, 267, 636-646.
42. Uddin, A.S.M.I.; Yaqoob, U.; Chung, G.-S. Dissolved hydrogen gas analysis in transformer oil using Pd catalyst decorated on ZnO nanorod array. *Sens. Actuator B-Chem.* **2016**, 226, 90-95.
43. Chen, W.; Zhou, Q.; Gao, T.; Su, X.; Wan, F. Pd-doped SnO_2-based sensor detecting characteristic fault hydrocarbon gases in transformer oil. *J. Nanomater.* **2013**, 2013, 9.
44. Chen, Z.; Zhang, X.; Xiong, H.; Chen, D.; Cheng, H.; Tang, J.; Tian. Y.; Xiao, S. Dissolved Gas Analysis in Transformer Oil Using Pt-Doped WSe_2 Monolayer Based on First Principles Method. *IEEE Access* **2019**, 7, 72012-72019.
45. Cui, H.; Zhang, X.; Zhang, G.; Tang, J. Pd-doped MoS_2 monolayer: A promising candidate for DGA in transformer oil based on DFT method. *Appl. Surf. Sci.* **2019**, 470, 1035-1042.
46. Zhang, Y.; Sun, X.; Tan, S.; Liu, T.; Cui, H. Adsorption characteristic of Rh-doped $MoSe_2$ monolayer towards H_2 and C_2H_2 for DGA in transformer oil based on DFT method. *Appl. Surf. Sci.* **2019**, 487, 930-937.
47. Delley, B. Dmol3 DFT studies: From molecules and molecular environments to surfaces and solids. *Comput. Mater. Sci.* **2000**, 17, 122–126.
48. Perdew, J.P.; Chevary, J.A.; Vosko, S.H.; Jackson, K.A.; Pederson, M.R.; Singh, D.J.; Fiolhais, C. Atoms, molecules, solids, and surfaces: Applications of the generalized gradient approximation for exchange and correlation. *Phys. Rev. B* **1992**, 46, 6671–6687.
49. Perdew, J. P.; Burke, K.; Ernzerhof, M. Generalized gradient approximation made simple. *Phys. Rev. Lett.* **1996**, 77, 3865-3868.
50. Grimme, S. Semiempirical GGA- type density functional constructed with a long- range dispersion correction. *J. Comput. Chem.* **2006**, 27, 1787-1799.
51. Monkhorst, H. J.; Pack, J. D. Special points for Brillouin-zone integrations. *Phys. Rev. B* **1976**, 13, 5188.
52. Hirshfeld, F. L. Bonded-atom fragments for describing molecular charge densities. *Theor. Chem. Acta* **1977**, 44, 129-138.
53. Ruiz-Puigdollers, A.; Gamallo, P. DFT study of the role of N-and B-doping on structural, elastic and electronic properties of α-, β-and γ-graphyne. *Carbon* **2017**, 114, 301-310.

54. Kang, B.; Lee, J. Y. Graphynes as promising cathode material of fuel cell: improvement of oxygen reduction efficiency. *J. Phys. Chem. C* **2014**, 118, 12035-12040.
55. Li, S. S. Semiconductor physical electronics. Springer Science & Business Media 2012.
56. Zhang, Y. H.; Chen, Y. B.; Zhou, K. G.; Liu, C. H.; Zeng, J.; Zhang, H. L.; Peng, Y. Improving gas sensing properties of graphene by introducing dopants and defects: a first-principles study. *Nanotechnology* **2009**, 20, 185504.
57. Patel, K.; Roondhe, B.; Dabhi, S.D.; Jha, P.K. A new flatland buddy as toxic gas scavenger: A first principles study. *J. Hazard. Mater.* **2018**, 351, 337-345.